

Southwest Consortium  
for  
Environmental Research and Policy;  
Final Report

Quantitative Analysis  
of  
Dynamic Video Images and Static Images  
of the  
El Paso del Norte Air Basin:  
Years 1992-1994

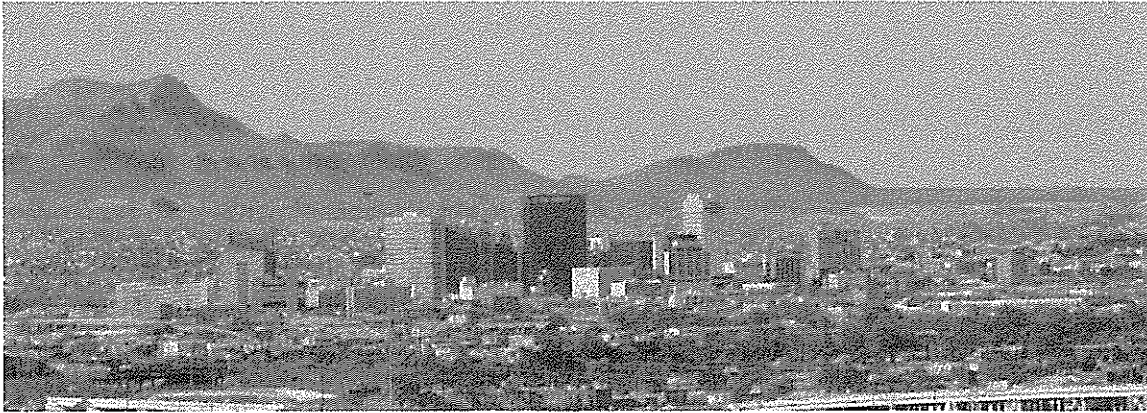
Principal Investigators for Project AQ95-1, CFDA No. 66.000

Charles D. Turner, Ph.D., P.E.  
Civil Engineering Department  
University of Texas at El Paso  
El Paso, TX 79968

and

Norris J. Parks, Ph.D.  
Civil Engineering Department, and  
Air Quality Research Group,  
Center for Environmental Resource Management  
University of Texas at El Paso, El Paso, Texas

August 15, 1997



## **The Goal: Clean Days in the Paso del Norte Air Basin**

### **Collaborating Investigators**

**N. J. Parks, C. D. Turner**

*Department of Civil Engineering, and  
Air Quality Research Group, Center for Environmental Resource Management  
University of Texas at El Paso, El Paso, Texas*

**S. L. Dattner**

*Monitoring Operations Division, Texas Natural Resource Conservation Commission  
Austin, Texas*

**J. A. VanDerslice**

*University of Texas Health Science Center at Houston,  
School of Public Health at El Paso  
Air Quality Research Group, Center for Environmental Resource Management,  
University of Texas at El Paso, El Paso, Texas*

**O. E. Chavez**

*Instituto Tecnológico y de Estudios Superiores de Monterrey,  
Cd. Juárez, Chihuahua, Mexico; and  
International City-County Management Association, USAID  
Washington, D.C.*

**A. G. Magratten, C. Saucedo**

*Department of Civil Engineering, and  
Air Quality Research Group, Center for Environmental Resource Management  
University of Texas at El Paso, El Paso, Texas*

**R. W. Gray**

*Institute for the Manufacturing and Materials Management  
University of Texas at El Paso, El Paso, Texas*

## TABLE OF CONTENTS

	PAGE
COLLABORATING INVESTIGATORS-----	ii
ABSTRACT -----	2
IMPLICATIONS -----	3
INTRODUCTION-----	3
MATERIALS AND METHODS -----	4
RESULTS -----	9
DISCUSSION-----	11
CONCLUSION-----	12
RECOMMENDATIONS-----	13
ACKNOWLEDGMENTS -----	14
REFERENCES -----	15
ABOUT AUTHORS-----	17
FIGURE AND TABLE CAPTIONS-----	18
TABLE 1-----	20
FIGURES ( APPENDIX I )-----	21

## ABSTRACT

Three years of video camera images encompassing about 90 square kilometers of the Paso del Norte Airshed, situated astride the U.S.-Mexico border and including the metropolitan areas of El Paso, Texas and Ciudad Juárez, Chihuahua, have been examined for years 1992-1994. For a selected, cloudless day, image set, quantitative analysis of time-lapsed, ambient aerosol images was accomplished using IMAGE software from U. S. National Institutes of Health. Each video image contained approximately 78 million volume elements (voxels) of data. Resolution of the analysis program was at the individual pixel and gray level intensity. A contrast parameter,  $C_{comp}$ , was calculated from intensities of adjacent, downtown — “dark” and “bright” — targets for the sunrise to ca. noon scattered light reaching the single camera video imager located 8 km away. Continual (1-hour average) PM-10 (<10  $\mu\text{m}$  aerodynamic diameter) concentration data was available from one monitoring station in the field of view. It was notable to observe that  $C_{comp}$ , derived from visible-range particle sizes (0.4-0.7  $\mu\text{m}$  diameter) explained about 40% of the variation in the ground station PM-10 data for the cloudless conditions of these initial investigations. The estimated variance ( $s^2$ ) about the mean line of maximum likelihood relating  $C_{comp}$  obtained from image analysis to ground station PM-10 values (for our single camera, single distance, set-up) increases in proportion to mean PM-10. The range of PM-10 values for  $0.1 < C_{comp} < 0.9$  in our study is ca.  $10 \mu\text{g}/\text{m}^3$  to  $120 \mu\text{g}/\text{m}^3$ ; the estimated PM-10 standard deviation ( $s$ ) for a nominal “clean” day at  $C_{comp} \approx 0.1$ :  $\text{PM-10} \approx 10 \mu\text{g}/\text{m}^3$  is ca.  $2 \mu\text{g}/\text{m}^3$  and on “dirty” days,  $C_{comp} \approx 0.9$ :  $\text{PM-10} \approx 120 \mu\text{g}/\text{m}^3$ ,  $s \approx 30 \mu\text{g}/\text{m}^3$ . These analyses indicate that variability of the PM-10 prediction from contrast measurements can be diminished by additional co-linear camera locations, closer proximity of the imaging “target” to continuous PM-10 monitors, and optical properties versus atmospheric particle size data. Available short range nephelometry, “visibility,” data compared favorably to the 8 km data.

## IMPLICATIONS

Poor air quality has brought the investigatory and regulatory attention of U.S. and Mexican federal, state, and municipal governments to bear on air pollution in the internationally situated Paso del Norte airshed because of attendant health effect issues. The measurements described here demonstrate the extraction of quantitative information from single camera airshed imaging (SCAI); potentially obviating the installation of new monitoring stations and improving resource allocation. The analytical approach described can correlate image contrast (a visibility index) with concentrations of visibility impairing, respirable particles. These images, which - when viewed dynamically - show particles arising and being transported are matched with existing data from ground monitoring stations in bordering Cd. Juárez and in El Paso.

## INTRODUCTION

Knowledge about sources and quantity of air contaminants in the Paso del Norte Airshed, which encompasses the area of metropolitan El Paso, Texas, Ciudad Juárez, Chihuahua, and Sunland Park, New Mexico, is essential to rational policy development and effective implementation of air quality control measures on both sides of the border.<sup>1</sup> Conventionally, this knowledge has been obtained by fixed-site continuous air monitors situated throughout the Paso del Norte Airshed.

The existence of three years of time-lapse video images taken every four seconds of the Paso del Norte Air Basin presented a unique opportunity to demonstrate alternative means to estimate PM-10. Earlier, Dattner showed, using 1990 dichotomous sampler data, that due to meteorological characteristics in the Paso del Norte Airshed, the major impairment to visibility is expected to be PM-10.<sup>2</sup> Concentrations of visibility impairing, respirable particles shown in these video images has been

correlated with existing data for particle concentrations with aerodynamic diameters  $\leq$  a 50% cut point of  $10\mu\text{m}$  (PM-10) for the Chamizal National Memorial monitoring station bordering Cd. Juárez and El Paso.

In this report, we evaluate the implementation of a visual remote sensing technique using readily available computer hardware and software to extract and archive quantitative information from Single Camera Airshed Imaging (SCAI) time-lapsed video data. We examined the hypothesis that contrast would be correlated at some level with observed PM-10 levels in the Paso del Norte Airshed; thereby permitting the use of contrast measurements from video images to give us current and retrospective information about PM-10 and co-varying pollutant concentrations ( particularly CO, Ozone) in the airshed.

## **MATERIALS AND METHODS**

### Imaging Equipment and Software.

The visual images examined were based on selected SCAI angles and fields of view that included downtown El Paso and the western half of Cd. Juarez (Figure 1). The camera faces southwesterly as shown on the map (Figure 2); images were captured every 4 seconds. During the early morning hours, scattered light from particles (nominally in the 0.1 to  $1\mu\text{m}$  range) of ambient aerosol in the lower portion of the Rio Grande Valley (part of the Paso del Norte airshed) reveals a notable inversion.

Video images were recorded by the TNRCC using a Panasonic Model WV-CL 704 security camera and a Panasonic Model AG-6720A-P time-lapse S-VHS recorder (S-VHS is a superior resolution video recording format which separates chromescence and luminescence). The images were then digitized using two Panasonic PV-S4566 S-VHS Video Cassette Recorders (Matsushita

Electric Corporation of America, Secaucus, NJ) as playback units and an Apple Power Macintosh 7100/80/CD/AV (Apple Computer Inc., Cupertino, CA), with built-in video digitizer.

The moving time-lapsed images were "captured" using FUSION RECORDER (Version 1.1; Videofusion, Inc., software, supplied by Apple Computer Inc). Capturing yields an 8-bit digital 640x480 pixel image with 256 intensity levels deep; thus each video time-lapsed image frame has 78,643,200 volume elements (voxels) of information.

The digitizer features automatic gain control and other image normalizing circuitry. The industrial security camera and time-lapse S-VHS video recorder that originally recorded the images also feature automatic light leveling capabilities in order to minimize extreme variations in image light intensities and preserve these intensities within the range of the video media. Correction for total light extinction was not possible due to the varying degree that the different equipment performs automatic light leveling. Intensity of the near foreground was used as an internal standard (Figure 1) with negligible effect assumed for varying PM-10 levels.

The image analysis software, IMAGE© (Rev. 1.59),<sup>3</sup> was acquired from the U. S. National Institutes of Health.

#### Particle Concentration (PM-10) Data.

The PM-10 data was extracted from TNRCC, El Paso City County Health and Environment Department (EPCCHED), and USEPA AIRS database archives that included criteria pollutant and meteorological data for days of interest.

The dynamic information from a continual (one-hour averaging) PM-10 monitor at the Chamizal National Memorial was uniquely necessary for the present analysis. The one-hour-average PM-10 monitor calibration rests on summations of the hourly values over 24 hours and comparisons to 24

hour integral PM-10 samplers in the same vicinity for discrepancies.<sup>4</sup> Absolute calibration for individual measurements with this instrument was implemented after the 1992 period we reported here.

In the analyses reported here, the light scattering parameter we quantify includes the influence of atmospheric and pollutant gases. Continuous data for other priority pollutants was available in 1992, but continuous PM-10 measurements that could be correlated with contrast ( $C_{comp}$ ) measurements were only available at the Chamizal site run by the EPCCHED (Figure 3). This allowed regression analysis to be performed for contrast versus PM-10 and other criteria pollutant data for the exact same days and time of day. In the data sets we examined, only the contrast versus PM-10 correlations were informative. During the period of our analysis, the quality assurance ranges for summations from the one-hour-averaging PM-10 sampler was in nominal agreement with 24-hr integrating samplers downtown near our contrast targets.

### Procedures.

The procedural task was to identify adjacent "bright" and "dark" targets (Figure 1) that would be quantifiable in terms of brightness or density (darkness) in the video images and useful for calculating contrast (C) ratios .

We first had to address issues relating to the volume of data contained on 32 tapes covering three partial years of video data is about 1.6 Terabytes or  $4 \times 10^{14}$  voxels. A winnowing process was used initially to extract a parsimonious image set that was judged adequate to demonstrate the utility of quantitative image analysis without exceeding available mass storage capacity. Video images pertaining to actual dates were surveyed qualitatively at first and classified into: "clean," (all details in background of image clear), "medium" (some details obscured), and "dirty" (many details obscured or lost).

After the selection criteria of same camera angle, good quality tapes, and available continuous PM-10 data, were met, useful data sets from the earliest period of the time-lapse video imaging project were identified. A set of images from 8AM to 12PM period during which the targets were fully illuminated for eleven days from Fall, 1992, that included a time segment where conditions were characterized as “dirty” were selected for analysis.

Reference targets within a few hundred meters of the camera were selected as internal controls. These references provide independent tracking of changes in intensity due to sun angle, possible tape quality variation, and various meteorological phenomena (cloud cover, precipitation, etc.) that may affect the primary target intensity values and contrast calculations. Tape quality is not a common problem but appeared occasionally.

The IMAGE<sup>©</sup> software allows sampling of image brightness or density based on a 256-level (gray) intensity scale at a given pixel site (Figure 3a-c). These intensity values can then be exported to a spreadsheet for subsequent contrast (visibility index) calculations. Intensity is given directly by the IMAGE<sup>©</sup> application as a value between zero and 255, with zero being lightest and 255 being darkest for each pixel.

For this work, we used the complement (brightness) scale with zero as black and 255 as maximum brightness. This conversion of directly observed intensities to complement numbers provides a mathematical convenience associated with avoiding zero as denominator.

Groups of nine pixels (about 15 X 15 meters-square on the target structures at 8 km) were selected at coordinates which were nominally in the same position for each captured image. Various experimental artifacts can have small effects on image registration. Elementary algorithms were constructed in spreadsheets to which the pixel intensity values were exported. These algorithms

identified the maximum intensity for the "bright" target and the minimum intensity for "dark" target. These values are the basis of  $I_{bright}$  and  $I_{dark}$  in Equation 1.

Various notation is found in the literature<sup>5, 6, 7</sup> but yield similar results — an index of 0 to 1 where 1 indicates high amounts of contrast and zero indicates minimal contrast. Contrast is then calculated according to the following formula:

$$C(x) = \frac{(I_{bright} - I_{dark})}{I_{bright}}$$

**Equation 1**

In this report, our results are presented using the complement,  $C_{comp}$ , of  $C(x)$  as defined in Equation. 2.

$$C_{comp} = 1 - C(x) = \frac{I_{dark}}{I_{bright}}$$

**Equation 2**

With this transformation, we were able to estimate least squares regression coefficients for each of the eleven days of data (Figure 6a and Table 1) with the constraint that the contrast parameter,  $C_{comp} = 0$  corresponded to PM-10 concentration = 0; thus, the regression slopes were estimated restricting the intercept parameter to zero and forcing each of the regression lines through the origin. While this approach ignores Rayleigh scatter, attributable to atmospheric gases, the effect was assumed to be negligible. Both the numerator and denominator of Equation. 2 are similarly varying (but opposite signs of the derivative) exponential functions of PM-10, thus yielding the observed linear relationship between  $C_{comp}$  and PM-10 concentration.<sup>8</sup>

Using the estimated regression coefficients, predicted PM-10 values were calculated for each of the 11 days of data for levels of  $C_{comp}$  ranging from 0.1 to 0.9. A mean of these predicted PM-10 values and a standard deviation were calculated for each value of  $C_{comp}$ . Based on the mean and standard deviation, distributions of the predicted PM-10 were computed at each value of  $C_{comp}$ . These distributions represent the expected variability associated with PM-10 predictions for any observed level of  $C_{comp}$  (Figure 7).

## RESULTS

### Ranges for one-hour average PM-10 Concentrations.

The result of the comparison between the qualitative analysis and mass measurements reveals the following: 1) dirty days were defined as those that had a peaks of  $\geq 90 \mu\text{g}/\text{m}^3$ , and 2) there is variation of PM-10 within a dirty day. Our computed  $C_{comp}$  results and available PM-10 data for a fall day, October 13, 1992, with the "dirtiest" time segment plotted as  $C_{comp}$  and PM-10 vs. Time-of-Day (8AM to 12PM) in Figure 4. It is apparent that there is appreciable temporal variation in PM-10 concentrations that are closely tracked by our computed  $C_{comp}$  values. It is important to note that without a one-hour-average PM-10 monitor (beta gauge), it would have been difficult to identify this correlation.

### Comparison to Continuous Nephelometry.

At particular junctures throughout the period of study, data was available from a TNRCC nephelometer which gave an alternative visibility index (range in kilometers) near our downtown targets.<sup>9</sup> Measuring scattered light at specific points, the device serves as a calibration for analysis of similar conditions using the digital transformation of video. The comparison between PM-10 and nephelometer results for a particular day during the study period is shown in Figure 5.

### Correlations of $C_{comp}$ to One-hour Average PM-10 Concentrations.

Correlations between PM-10 data provided by the beta gauge located 3.5 km away at the Chamizal National Memorial (U.S. Park Service) (Figure 1 and 2) and contrast data extracted from the videotapes are shown for a series of "dirty" days showing similar slopes and predictive capabilities (Figure 6a). The individual slopes for the regression fits in Fig 6a are given in Table 1.

In Fig. 6b, all the data points taken from the hours 8AM-12PM for the dates in Table 1 are plotted. The least squares regression line was forced through the origin and gives a slope very similar to the mean of the least squares fits to the data for each day individually (Fig. 6a).

Distributions of predicted PM-10 values of  $C_{comp}$  ranging from 0.1 to 0.9 are presented in Figure 7 for each 0.1 increment of  $C_{comp}$ . As the level of observed contrast decreases (i.e.  $C_{comp}$  increases), the variability in the predicted PM-10 increases. This pattern is due in part to the estimation process which forced the regression lines to pass through the origin. As a result of this restriction, there is no calculated variability in the predicted PM-10 values at  $C_{comp} = 0$ . In the actual atmospheres we have observed, this limit is not approached and we have measured values and calculated variances for the typical lower limit of  $C_{comp} \approx 0.1$

At the other limiting extreme, the increase in variability is directly related to the fact that  $I_{bright}$  is approaching  $I_{dark}$ . Experimentally, we are measuring a difference that is approaching zero and a ratio that is approaching 1.0. As the value of  $C_{comp}$  defined by Equation. 2 approaches 1, very large variation in PM-10 has very little effect on  $C_{comp}$ . In general, when PM-10 is greater than the upper limit that yields  $C_{comp} = 1$ , any value of PM-10 will yield  $C_{comp} = 1$  and the variance becomes infinite. For reference in Fig. 7,  $C_{comp} = 1$  represents the complete absence of contrast between a black target and a white one. The limit of useful range in this study is  $C_{comp} \approx 0.9$ ; PM-10

$\approx 120 \mu\text{g}/\text{m}^3$ . The extrapolated range in Figure 6b and in Figure 7 for  $C_{comp} = 1$  is the slope, i.e.  $126 \pm 30 \mu\text{g}/\text{m}^3$ .

## DISCUSSION

The main issue is whether the hypothesis has been supported or rejected. The hypothesis is that the use of contrast measurements from video images can provide useful estimates of PM-10 levels in the Paso del Norte Airshed for conditions similar to our selected "cloudless" day data set. First we note that days characterized by "inversion" pollution and typically high ozone levels as well as PM-10 fall into this category. Then we further note the t-statistic and the "p" values of Table 1. The slopes of the regression lines associating  $C_{comp}$  and PM-10 concentration are highly significantly different from zero.

As can be seen graphically from Figures 6a, 6b, and 7, the variability of reported PM-10 concentrations from continuous beta gauge measurements is a function of the  $C_{comp}$  value. Even at the highest  $C_{comp}$  value (0.9), the variability about the predicted mean PM-10 value is insufficient to reject the hypothesis that  $\bar{C}_{comp}$  is dependent on PM-10 levels in the Paso del Norte Airshed for the conditions we examined.

This variability is a result of several factors. An important factor is likely the relatively large distance (3.5 km) between the one-hour-average PM-10 monitor and the targets and the spatial non-uniformity across the air basin of the light scattering particle concentrations. Additional variability can be attributed to chemical and elemental composition of the particles. The influence of these factors on bulk light scattering properties of the ambient aerosol is inferred from Dattner's<sup>2</sup> 1990 study which showed variation in chemistry of PM-10 and particle size distribution.

Particle size distribution effects on the variability are expected. Our video images are only imaging a light wavelength window corresponding to light scattering by particles in the fine particle fraction on the order a few tenths of a micrometer diameter whereas the available particle concentration data includes everything up to 10  $\mu\text{m}$ .

## CONCLUSION

From this investigation it is clear that "off the shelf" technology is available to conduct useful visibility analysis of air pollution in a semi-arid, mountain valley, airshed. We found this to be the case despite the limitations of a single camera, non-adjacent one-hour-average PM-10 monitors or no particle size distribution data from instruments for days with anomalous visibility conditions.

Advances in technology are expected to facilitate the collection and analysis of visibility data, allowing greater precision. The computers used for this work have been superseded by higher performance units that are have lower cost. By optimizing the acquisition and analysis steps, we anticipate that such analyses can be done by one person remotely and in a relatively short time frame. The quantitative data gathering techniques described herein in terms of "proof of principle," indicate that readily available resources and technology for remote sensing may present an alternative means for many municipalities charged with monitoring and managing an airshed.

In addition, it is anticipated that in future work, the USEPA sponsored El Paso Summer Ozone Study of 1996 will provide useful corollary data in the form of broader measurement of priority pollutants to co-vary with PM-2.5 and PM-10 and, ideally, additional nephelometry sites for comparison to the Long Range SCAI and MCAI technology described herein that looks at many cubic kilometers of ambient aerosol at any given time.

## RECOMMENDATIONS

The constraints of SCAI are the two dimensional perspective and sun angle in relation to the targets limiting the duration reflected light is available for contrast analysis. To extend usefulness, current extensions of this methodology utilize a multiple camera airshed imaging (MCAI) approach and include the addition of optics for evaluating the utility of light polarization<sup>10, 11, 12</sup> analysis or other optical phenomena. With more beta gauges and nephelometers located in various parts of the airshed, adjacent targets can be sought and used with confidence that they will track PM-10 levels closely with the gauge. This allows more effective resource management because several sets of targets may be monitored simultaneously, especially when maintaining a wide angle of view on all cameras. MCAI is made more important by the USEPA announced PM-2.5 standard, because light scattering is dominated by the fine particle, PM-2.5 component of PM-10.

## ACKNOWLEDGMENTS

This study was supported in part by the Southwest Center for Environmental Research and Policy (SCERP), Project No. AQ95-1, CFDA No. 66.000, administered by the Center for Environmental Resource Management (CERM), University of Texas at El Paso. We also acknowledge uniquely valuable contributions of Joe Saenz, Archie Clouse, Rose Irizarry, Brian Lambeth, and Dee Moss of TNRCC; Henry del Rio and Jesus Reynoso of EPCCHED; Ing. Oscar Ibañez Hernández of the Dirección de Desarrollo Urbano y Ecología, Cd. Juárez, Chihuahua (DDUE); Josephine Ball and Eric Aaboe of the New Mexico Environment Department (NMED); and Robert Currey at UTEP/CERM. Nancy Judith Castro, Elsa Tarin, Ruben Orquiz -Department of Civil Engineering (UTEP).

## REFERENCES

1. "La Paz Agreement," Agreement between the United States of America and the United Mexican States on Cooperation for the Protection and Improvement of the Environment in the Border Area. Appendix I, Annex V. Signed August 14, 1983, TIAS 10827.
2. Dattner, Stuart L., Air Quality Assessment Program: El Paso/Juarez 1990 PM-10 Receptor Modeling Feasibility Study; Texas Natural Resource Conservation Commission: Austin, TX, December 1994; AS-43.
3. IMAGE (Rev 1.59), U. S. National Institutes of Health (Current Rev. available on the World Wide Web at <http://rsb.info.nih.gov/nih-image/>, and is available via anonymous FTP from [zipper.nimh.nih.gov](http://zipper.nimh.nih.gov), or on floppy disk from the *National Technical Information Service, Springfield, Virginia, part number PB95-500195GE1.*), 1996.
4. Del Rio, Henry. Private Communication. El Paso City-County Health and Environment Department. El Paso, Texas. June 19, 1996.
5. Seinfeld, John H. *Atmospheric Chemistry and Physics of Air Pollution* ; Wiley and Sons, New York, 1986; pp. 289-306.
6. Cooper, C.D.; Alley, F.C. *Air Pollution Control* ; Waveland Press, Inc, Prospect Heights, IL 1994; pp. 42-69.
7. Boubel, R.; Fox, D; Turner, D.; Stern, A. *Fundamentals of Air Pollution*. 3rd Ed., Academic Press, San Diego, 1994; 195-228.
8. Waggoner, A.P., Weiss, R.E., Ahlquist, N.C., Covert, D. S., Strad, W., Charlson , R.J.; *Atmos. Envir.* 1981, 15, 1891-1909.
9. Lambeth, B. Private Communication. Texas Natural Resources Conservation Commission. Austin, Texas. January 17, 1996.

10. Baines, S. Sunfish Shows Way Through the Fog; *Science*. 1996, 272, 653.
11. Tyo, J.S., M.P. Rowe, E.N. Pugh, Jr., and N. Engheta. Target Detection in Optically Scattering Media by Polarization-Difference Imaging. *Applied Optics*, Vol. 35, No. 11, 10 April 1996.
12. Egan, W. G., *Photometry and Polarization in Remote Sensing*, (Elsevier, New York) 1985.

## ABOUT THE AUTHORS

N. J. Parks is an Adjunct Professor, and C. D. Turner is a Professor in the Department of Civil Engineering, E-201, University of Texas at El Paso, El Paso, Texas 79968-0516; S. L. Dattner is a Senior Atmospheric Scientist for the Texas Natural Resource Conservation Commission, Monitoring Operations Division, MC-165, P.O. Box 13087, Austin, Texas 78711-3087. J. A. Vanderslice is the Acting Program Director of the University of Texas - Houston School of Public Health at El Paso, 1100 N. Stanton, Suite 110, El Paso, TX 79902; O. E. Chavez is a Resident Advisor for the International City/County Management Association (USAID Contract), a Paso del Norte Air Quality Task Force (El Paso, Texas and Cd. Juárez, Chihuahua) member, and an Environmental Scientist for the Instituto Tecnológico y de Estudios Superiores de Monterrey (ITESM), Campus Ciudad Juárez, Avenida Tomás Fernández, Cd. Juárez, Chihuahua, Mexico, CP 32320; A. G. Magratten and C. Saucedo are student research assistants in the Air Quality Research Laboratory, Department of Civil Engineering, E-201, University of Texas at El Paso, El Paso, Texas 79968-0516; R. W. Gray, Computational Systems Specialist, Institute of Manufacturing and Materials Management; and Center for Environmental Resource Management, Room 401 Burgess Hall, W. University Avenue, University of Texas at El Paso, El Paso, Texas 79968.

## FIGURE AND TABLE CAPTIONS

**Figure 1.** Typical 1992 Camera View of Paso del Norte Airshed with landmarks labeled.

**Figure 2.** Location of the Paso del Norte Airshed showing camera position during study period, approximate field of view, visibility targets, continuous PM-10 monitor.

**Figure 3.** Zooming Capabilities of NIH Image. (a) The 1992 view of the airshed with the downtown target area selected. (b) The selection magnified once. (c) The selection magnified twice arriving at the one-pixel level.

**Figure 4.** PM-10 and  $C_{comp}$  profiles for October 13, 1992.

**Figure 5.** PM-10,  $C_{comp}$ , and Nephelometer profiles for October 17, 1992. Axis A is the result of the computation derived from Equation 2. Axis B is derived from the complement of Nephelometer data;  $R_{comp} = 1 - (\text{Range in km}/10)$ .

**Figure 6a.** Least squares regression lines for PM-10 vs.  $C_{comp}$  for eleven dirty days individually, during Fall 1992. The mean of the best fit lines (- - -) is computed from the mean of PM-10 predicted values at each  $C_{comp}$  value.

**Figure 6b.** Composite PM-10 vs.  $C_{comp}$  data for eleven days during Fall 1992 with least squares regression line forced through the origin.

**Figure 7.** Variability of the predicted PM-10 values at various *Ccomp* intervals based on the mean of the best fit lines from Figure 6a.

**Table 1.** Statistical tests for the significance of slopes from regressions shown in Figure 6a.

**Table 1.** Statistical tests for the significance of slopes from regressions shown in Figure 6a.

Day	Slope estimate	t-statistic	P-value
All	121	17.0	0.0001
September 3	170	11.3	0.0003
September 18	98	5.4	0.0056
October 3	108	4.3	0.0126
October 5	109	6.2	0.0034
October 6	117	3.2	0.0318
October 13	170	10.2	0.0005
October 17	96	10.6	0.0004
November 7	107	4.7	0.0092
November 8	74	5.1	0.0071
November 13	157	5.6	0.0052
November 14	178	10.0	0.0006

# APPENDIX I

## FIGURES

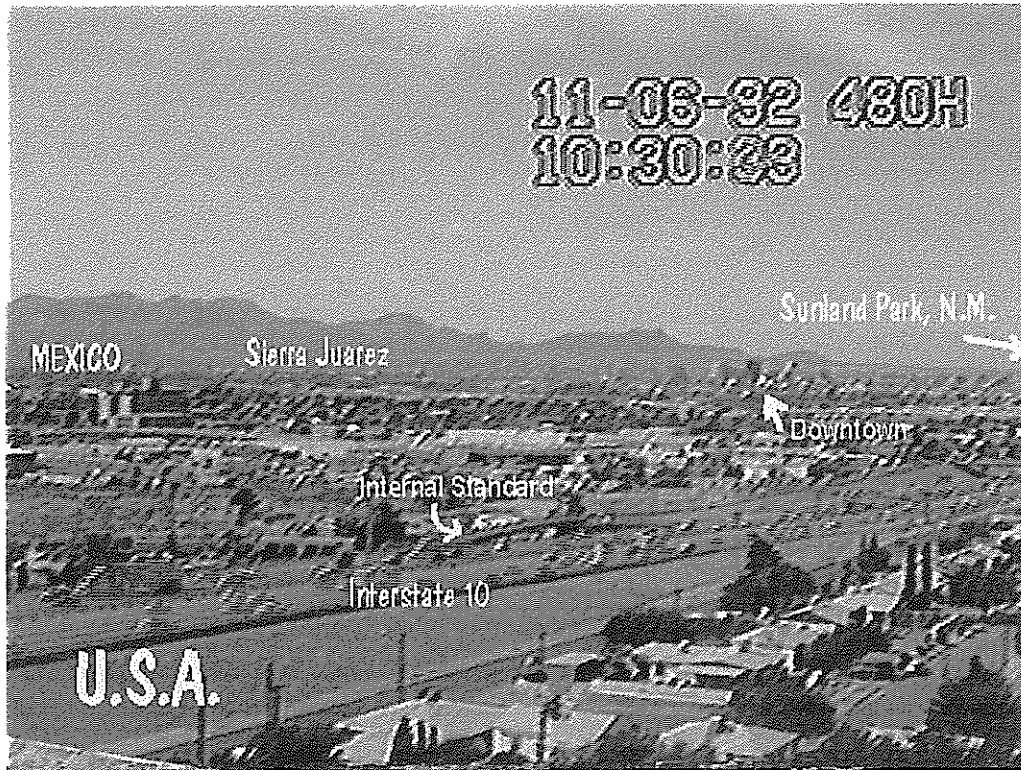
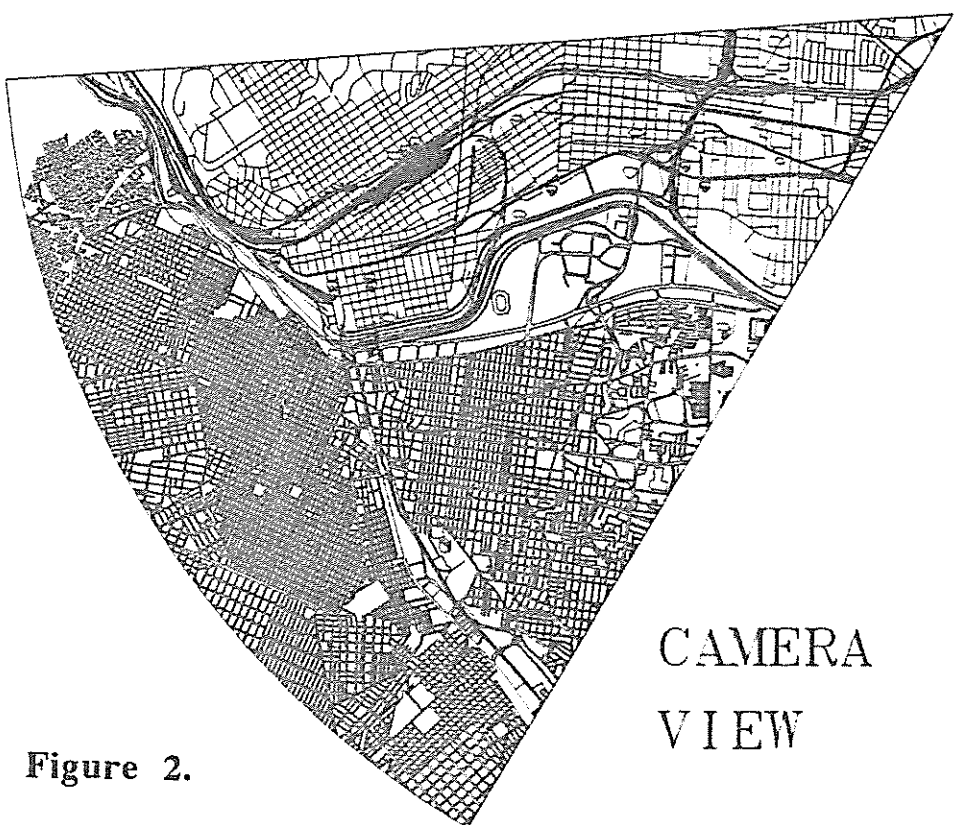
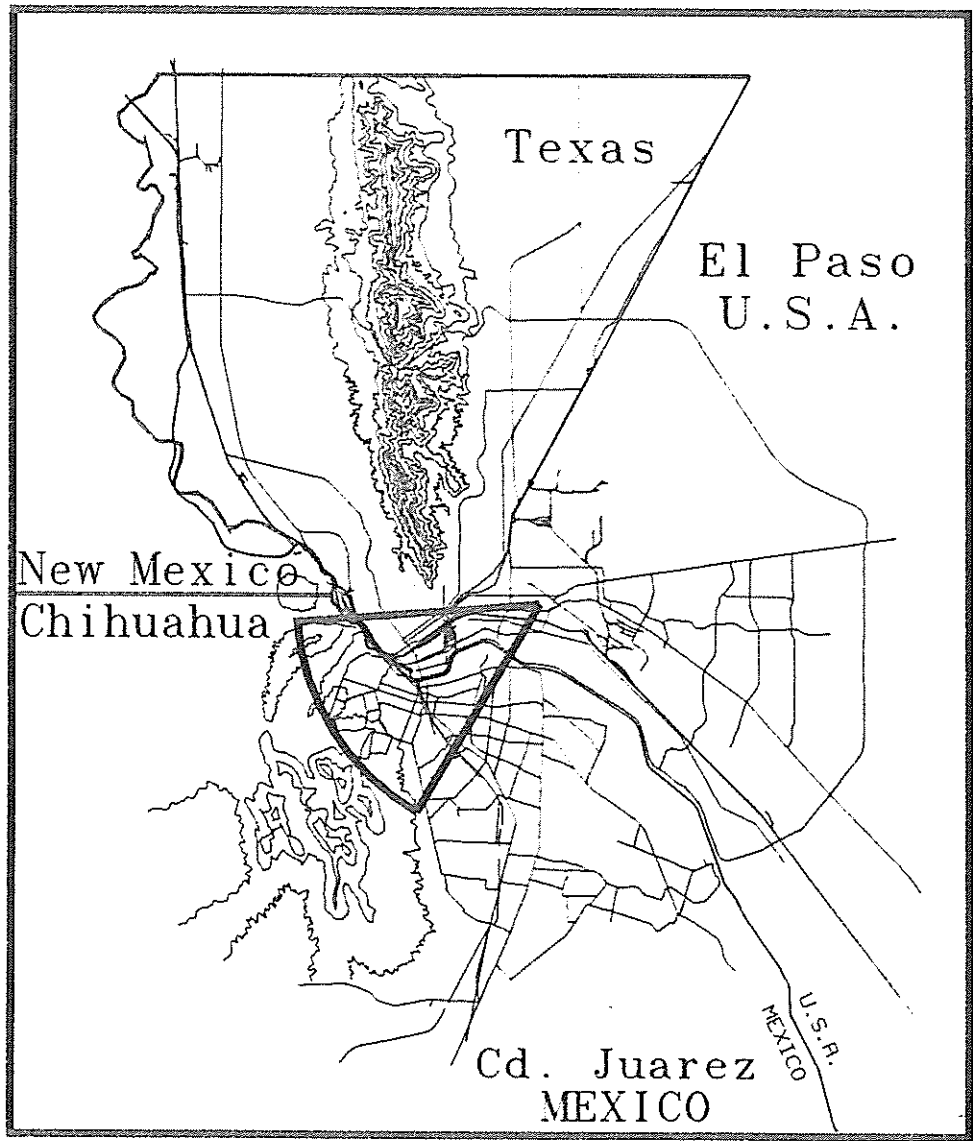


Figure1. The current westerly view with topographical features. Projected new camera sites are on Ranger Peak (2000 ft. higher in the Franklin Mountains with a southerly view) and off the left in Mexico with a north view. Landmark labeled "Downtown" is the site of "white" target and "black" target of the "two-target" contrast evaluation and is 8 km distant.



CAMERA  
VIEW

Figure 2.

**Figure 3.** Zooming Capabilities of NIH Image. (a) The 1992 view of the airshed with the downtown target area selected. (b) The selection magnified once. (c) The selection magnified twice arriving at the one-pixel level.

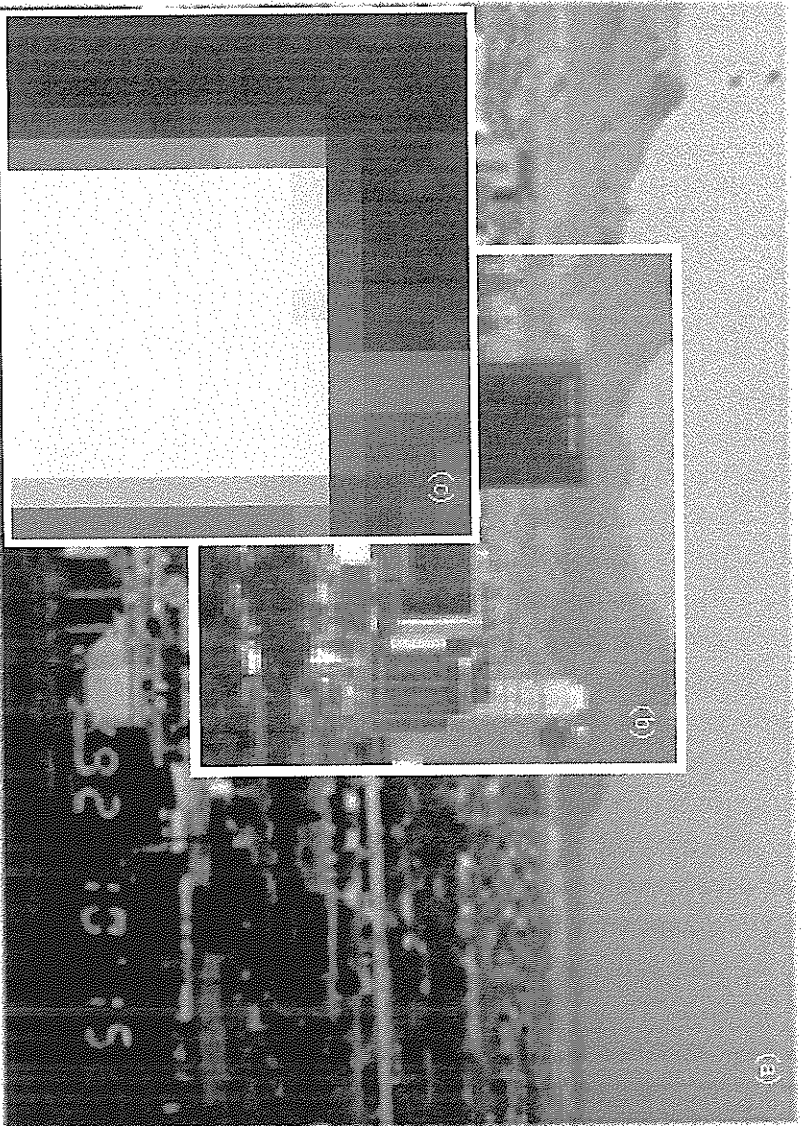
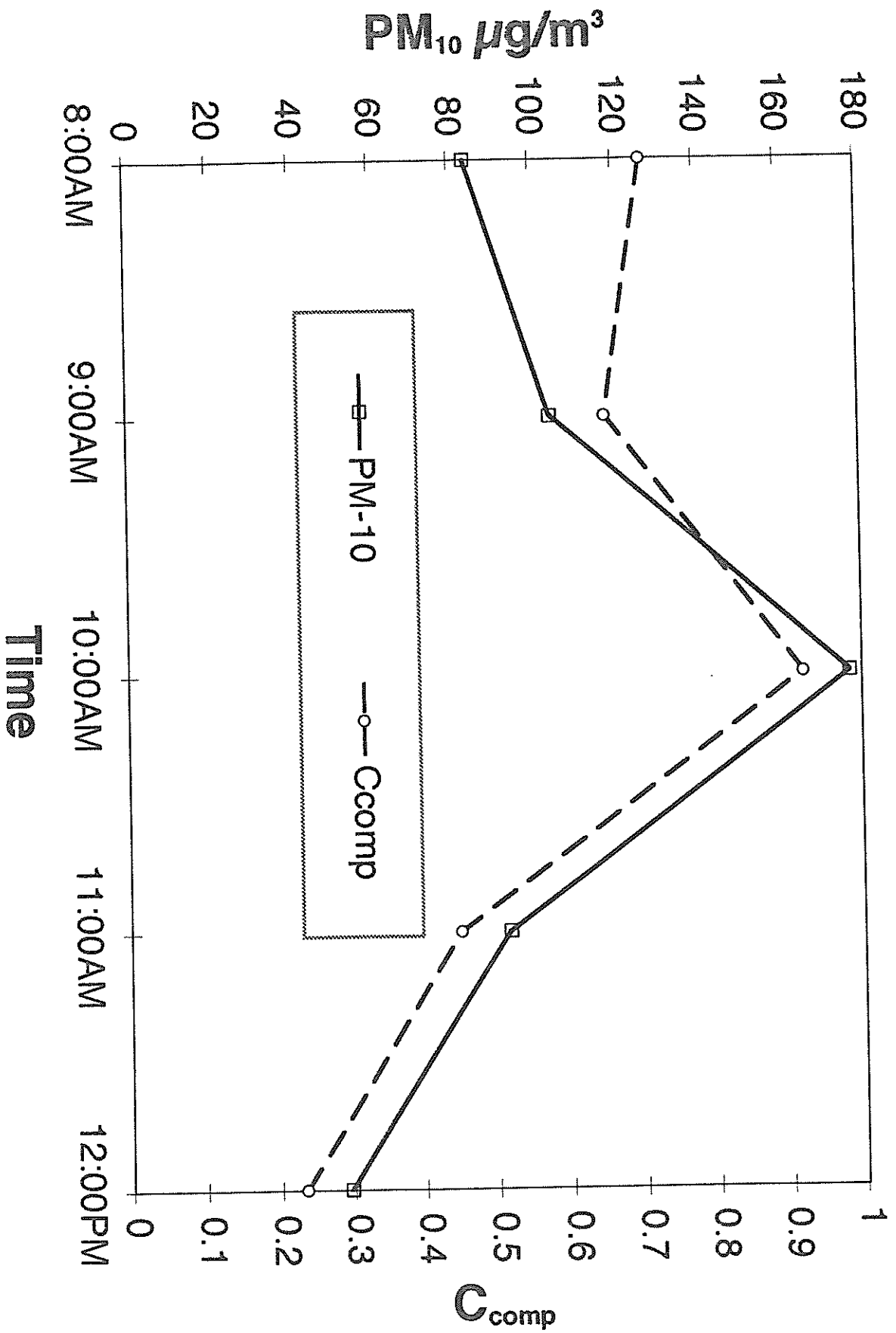


Figure 4



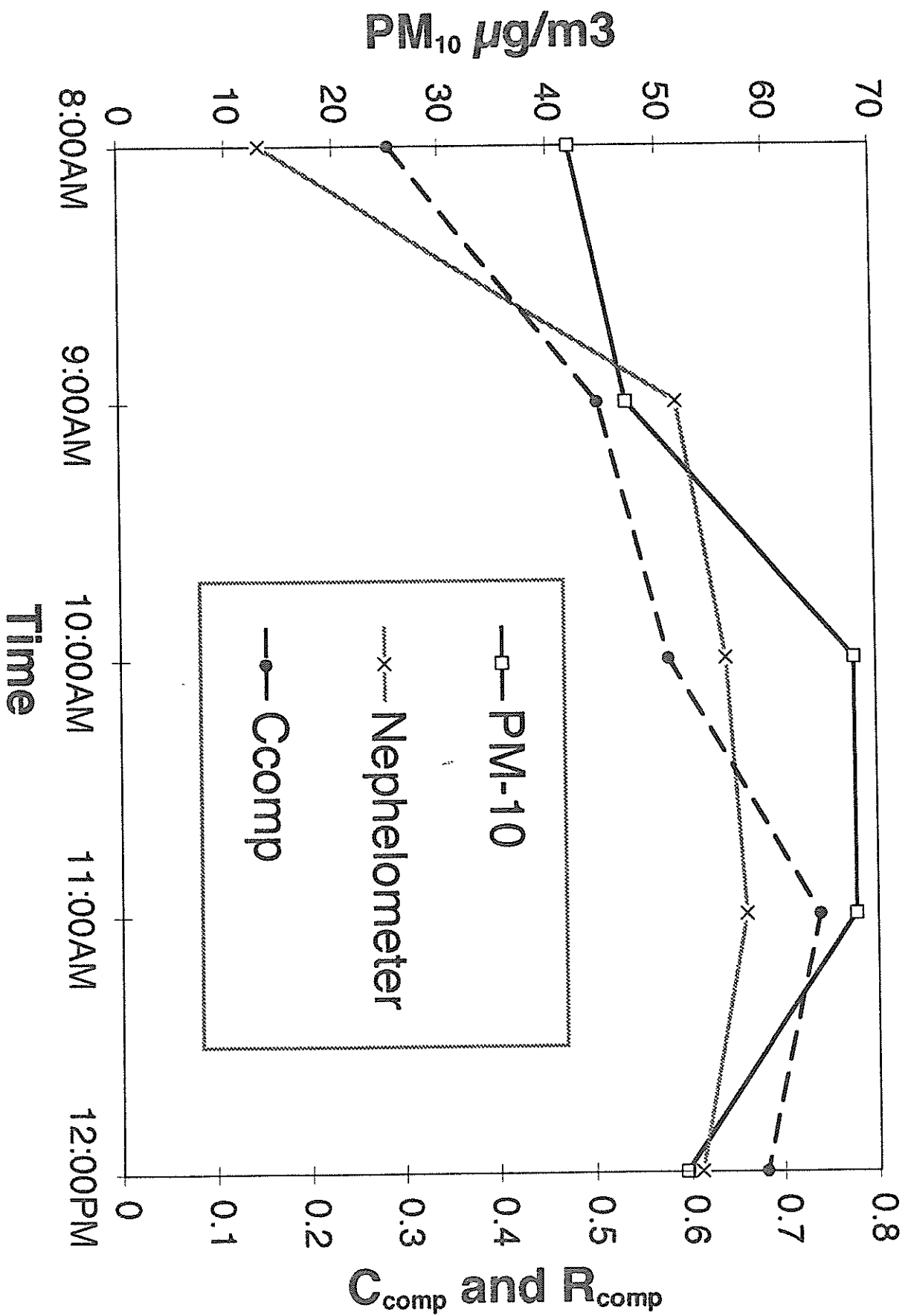
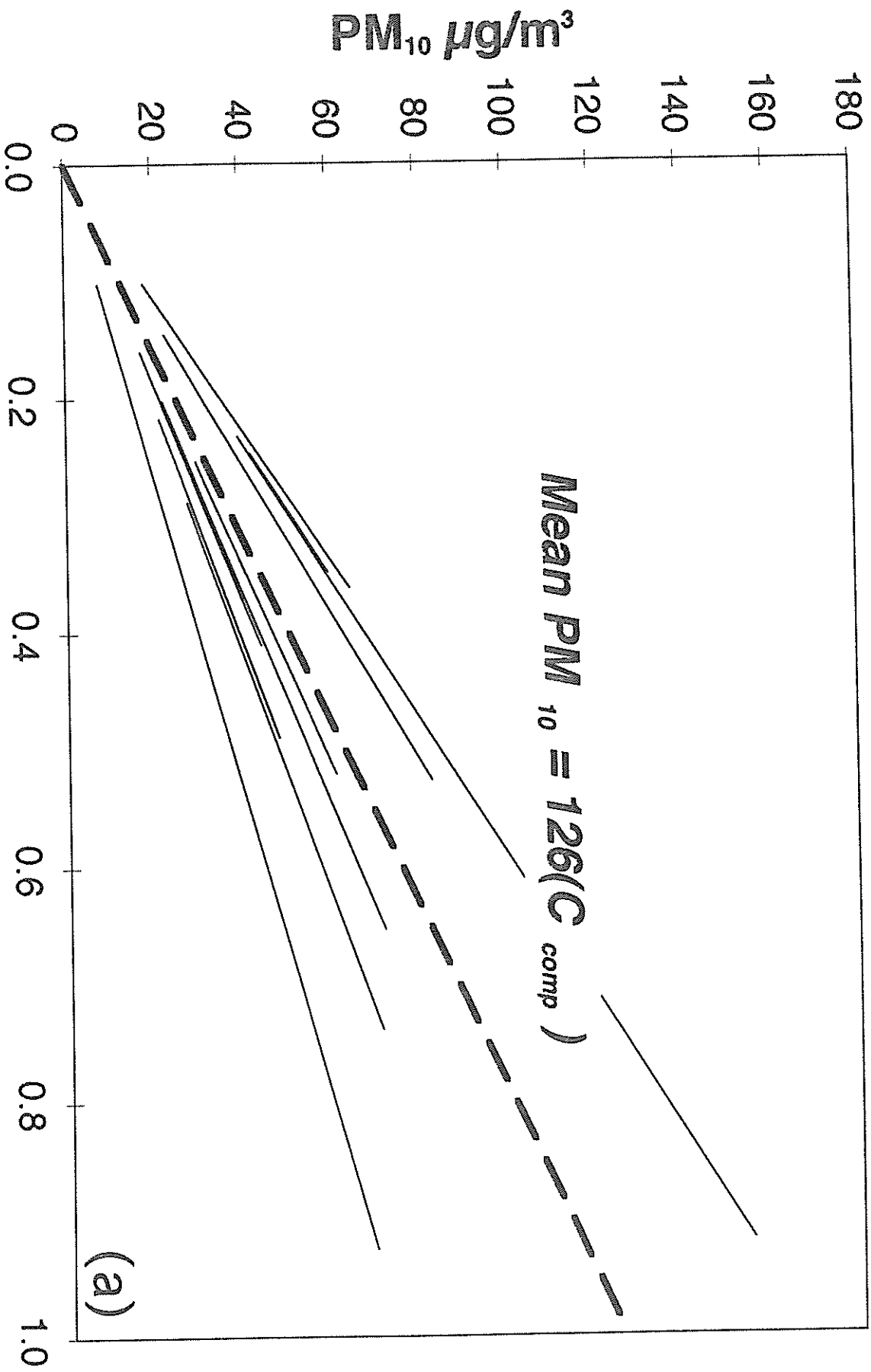


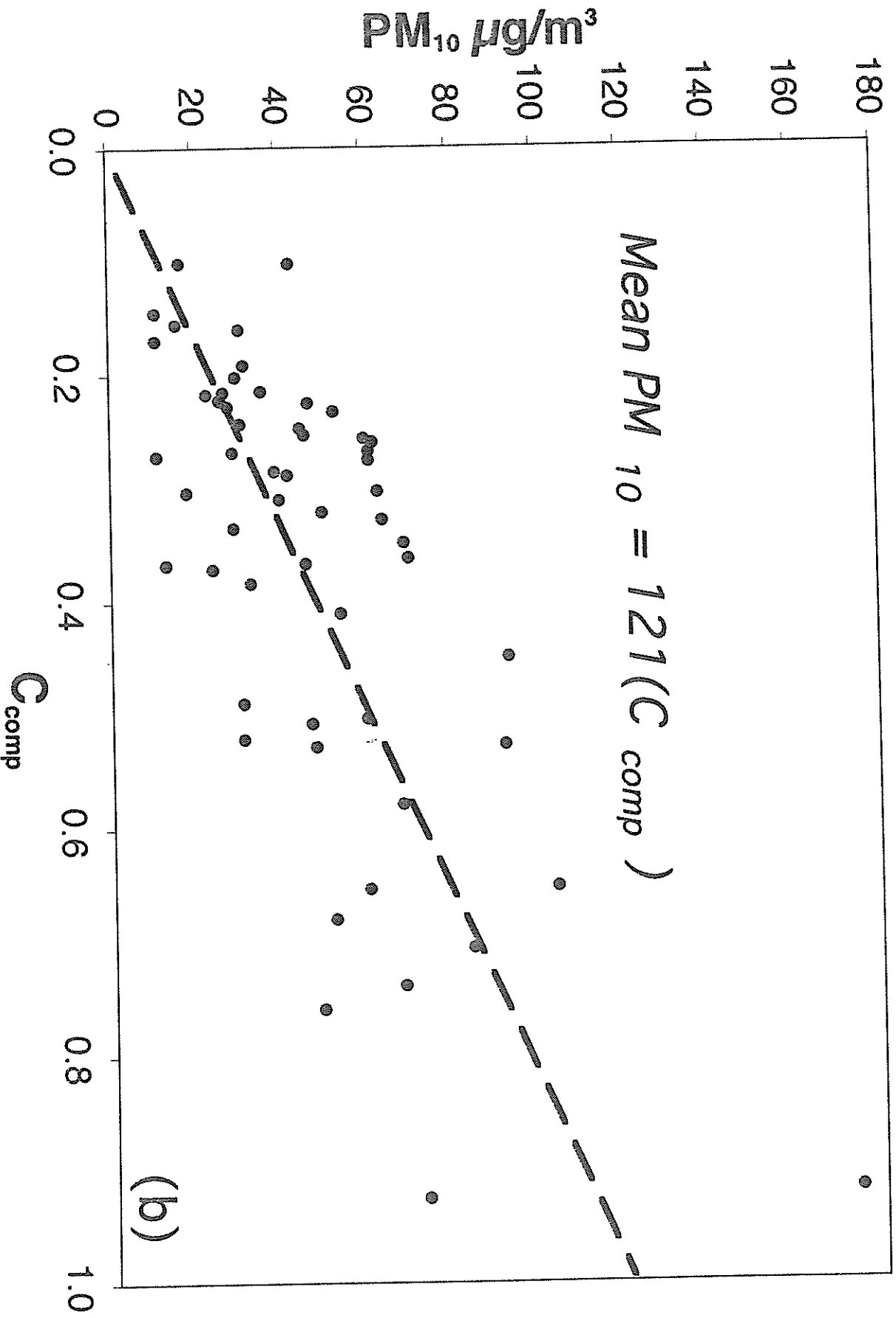
Figure 5

Figure 6a



(a)

Figure 6b



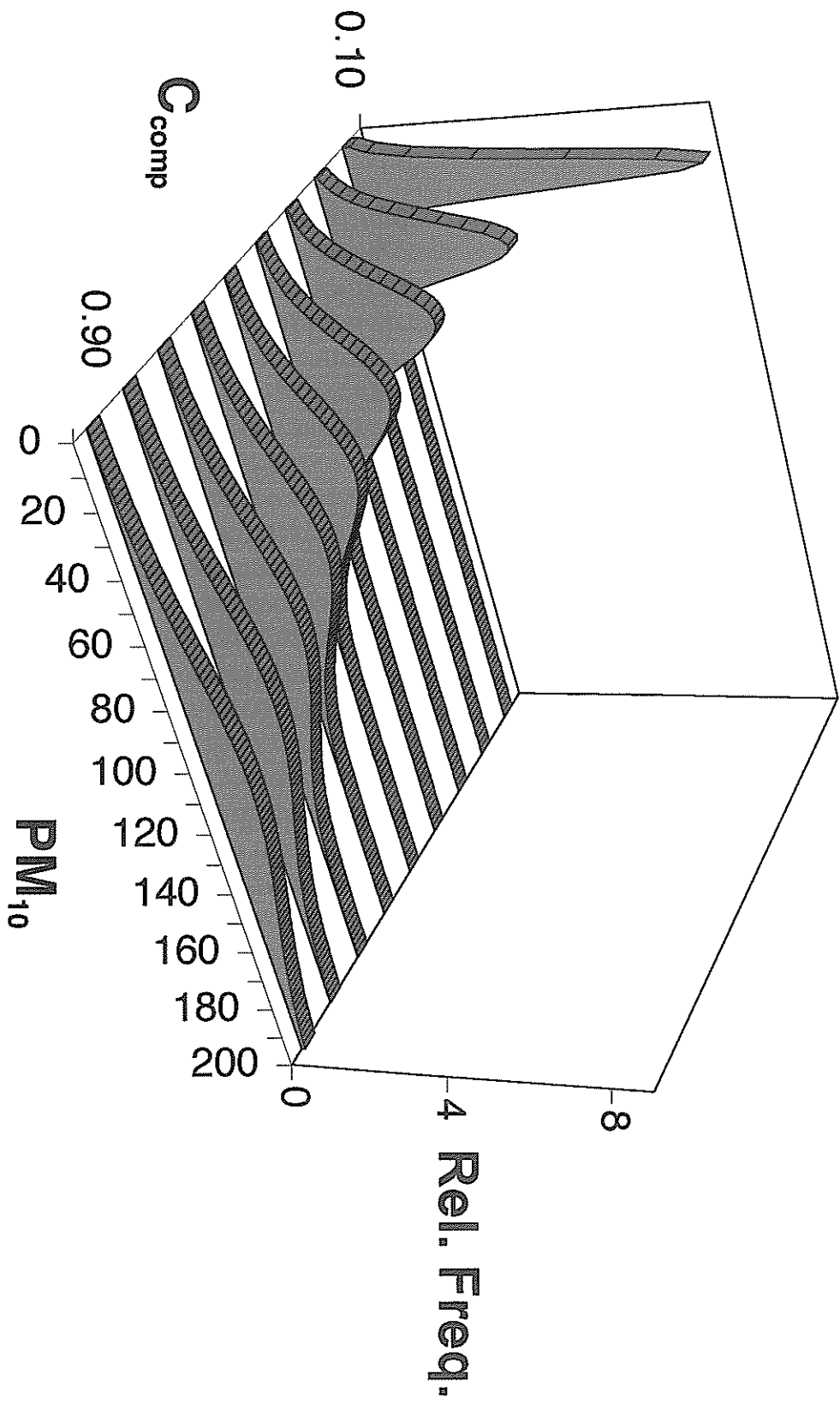


Figure 7

FINE FIBERS NUMBERS	TYPE	RING WT (G)	ERR	FILTER WEIGHT (G)		ERR	SAMPLE WT. (G)	SAMPLE WT (mg)	ERR	DATE	SAMPLING TIME	
				BEFORE SAMPLING (AVG)	AFTER SAMPLING							
13	Teflon	4.5863	(-1)	0.1075	0.1078	(-1)	0.0004	0.4	(-1)	11/12/97-12/97	R overlapped with #13 R run for 12 hrs	24.92877493
12	Teflon	4.5835	(-1)	0.1093	0.1046	(-1)	0.0011	1.1	(-1)	11/13/97-12/5/97	Midnight 13th-Midnight 5th (r. run every Friday for 24 hrs)	22.70299145
7	Teflon	4.5271	(-1)	0.1093	0.1079	(-1)	0.0016	1.6	(-1)	11/15/97-12/7/97	Midnight 14th-Midnight 7th (run all sat. & sun. for 48 hrs)	52.05333333
5	Teflon	4.5464	(-1)	0.1045	0.1077	(-1)	0.0032	3.2	(-1)	11/17-12/8/97	Midnight 16th-Midnight 8 (run all mondays for 24 hrs)	60.09615385
13	Teflon	4.5383	(-1)	0.1091	0.1083	(-1)	0.0002	0.2	(-1)	10/31-11/01/97	Midnight 31th-Midnight 01 (24 hrs)	
21	Teflon	4.5328	(-1)	0.1073	0.1075	(-1)	0.0003	0.3	(-1)	11/01-02/97	Midnight 1th-Midnight 2th (24 hrs)	
5	Teflon	4.5398	(-1)	0.108	0.1064	(-1)	0.0005	0.6	(-1)	11/02-03/97	Midnight 2th-Midnight 3th (24 hrs)	
3	Teflon	4.3811	(-1)	0.107	0.1108	(-1)	1E-04	0.1	(-1)	11/04-05/97	Midnight 4th-Midnight 5th (24 hrs)	
13	Teflon	4.5363	(-1)	0.1092	0.1095	(-1)	0.0003	0.3	(-1)	11/05-05/97	Midnight 5th-Midnight 6th (24 hrs)	
17	Teflon	4.5478	(-1)	0.1092	0.1073	(-1)	0.0011	1.1	(-1)	11/6-7/97	Midnight 6th-Midnight 7th (24 hrs)	
3	Teflon	4.3811	(-1)	0.107	0.1073	(-1)	1E-04	0.1	(-1)	11/11/97-12/97	It overlapped with #13 R run for 24 hrs	
13	Teflon	4.5363	(-1)	0.1092	0.1095	(-1)	0.0003	0.3	(-1)	11/13/97-12/5/97	Midnight 13th-Midnight 5th (r. run every Friday for 24 hrs)	
12	Teflon	4.5188	(-1)	0.1105	0.1112	(-1)	0.0006	0.6	(-1)	11/13/97-12/7/97	Midnight 14th-Midnight 7th (run all sat. & sun. for 48 hrs)	
7	Teflon	4.3781	(-1)	0.1061	0.1123	(-1)	0.0062	6.2	(-1)	11/15/97-12/7/97	Midnight 14th-Midnight 7th (run all sat. & sun. for 48 hrs)	
8	Teflon	4.5831	(-1)	0.1083	0.1095	(-1)	0.0013	1.3	(-1)	11/17-12/8/97	Midnight 16th-Midnight 8 (run all mondays for 24 hrs)	